ELSEVIER

Journal of Alloys and Compounds 408–412 (2006) 474–479

Journal of ALLOYS AND COMPOUNDS

www.elsevier.com/locate/jallcom

Growth and piezoelectric properties of $R_3Ga_5SiO_{14}$ and $RCa_4O(BO_3)_3$ (R: rare-earth elements) single crystals

Hiroaki Takeda [a,*], Hiroshi Nakao [b], Shintaro Izukawa [a], Hiroyuki Shimizu [a], Takashi Nishida [a], Soichiro Okamura [a], Tadashi Shiosaki [a]

[a] *Graduate School of Materials Science, Nara Institute of Science and Technology, 8916-5 Takayama-cho, Ikoma, Nara 630-0192, Japan*

[b] *Research and Development Division, Sakai Chemical Industry Co. Ltd., 5-1 Ebisujima-cho, Sakai, Osaka 590-0985, Japan*

Received 30 July 2004; received in revised form 15 December 2004; accepted 15 December 2004
Available online 13 June 2005

Abstract

$R_3Ga_5SiO_{14}$ (*R*GS, *R*: rare-earth elements) and $RCa_4O(BO_3)_3$ (*R*COB) single crystals were synthesized by the Czochralski technique and their piezoelectric properties were investigated. The piezoelectric moduli, d_{11} and d_{14}, of $La_3Ga_5SiO_{14}$ are higher than those of $Nd_3Ga_5SiO_{14}$. Moreover, in the *R*GS-type crystal, we found that the piezoelectric modulus, d_{11}, increased with the lattice parameter a. The ionic size preferences of all cation sites in the *R*GS-type structure were also clarified. Based on these results, a new *R*GS-type $Ba_3TaGa_3Si_2O_{14}$ crystal was synthesized. We have successfully grown *R*COB (*R* = La, Nd, Gd, Dy, and Y) single crystals with 1 and 2 in. diameter dimensions. The surface acoustic wave (SAW) properties of *R*COB filters were investigated. In *R*COB, the NdCOB single crystal showed the highest electromechanical coupling factors and lowest temperature coefficient of delay of the *R*COB crystals.
© 2005 Elsevier B.V. All rights reserved.

Keywords: Crystal growth; Piezoelectricity; Rare-earth element; Gallate; Borate

1. Introduction

Recent progress in electronic technology requires new piezoelectric crystals with a high thermal stability of frequency and high electromechanical coupling factors. For designing devices such as filters with a wide pass band while maintaining high stabilities and a small insertion attenuation, the necessity has arisen to develop new piezoelectric crystals having intermediate properties between those of quartz and lithium tantalate ($LiTaO_3$). Litium tetraborate ($Li_2B_4O_7$; abbreviated as LBO) and α-$AlPO_4$ have been candidates to satisfy these requirements [1]. Actually, LBO wafers have been mass-produced for use in intermediate frequency-surface acoustic wave (IF-SAW) devices. However, these crystals still have some disadvantages for mass-production. In LBO, a very low growth rate (<1 mm/h) is needed to produce inclusion-free crystals [2]. α-$AlPO_4$ and $GaPO_4$, which are polymorphs of quartz, also have significant technological growth difficulties and twinning problems [3]. This suggests that more detailed investigations are indispensable for the growth of bulk single crystals with high quality.

For new piezoelectric materials, we have focused on the rare-earth element-based single crystals such as $R_3Ga_5SiO_{14}$ (*R*GS, *R*: are rare-earth elements) and $RCa_4O(BO_3)_3$ (*R*COB). $La_3Ga_5SiO_{14}$ (LGS) is one of candidates to satisfy the requirements mentioned above [4]. Very recently, for use in a wideband-code division multiple access (W-CDMA) station, surface acoustic wave (SAW) filters made of LGS wafers have been mass-produced. Moreover, temperature and/or pressure sensors are being fabricated using LGS. The *R*COB have been developed which exhibit excellent non-linear optical properties and can be grown by the Czochralski (Cz) technique at a low cost [5–8]. The effective nonlinear coupling

* Corresponding author. Tel.: +81 743 72 6063; fax: +81 743 72 6069.
E-mail address: hiro-t@ms.naist.jp (H. Takeda).

0925-8388/$ – see front matter © 2005 Elsevier B.V. All rights reserved.
doi:10.1016/j.jallcom.2004.12.108

coefficient, d_{eff} = 1.1 pm/V, of $YCa_4O(BO_3)_3$ (YCOB) is greater than those of KH_2PO_4 and LiB_3O_5 (d_{eff} = 0.38 and 0.68 pm/V, respectively) from which bulk crystals can be easily grown [9]. This report has led to the study of *R*COB crystals as piezoelectric materials. In this paper, we demonstrate the successful growth of *R*GS and *R*COB single crystals by the Cz technique and disclose their piezoelectric properties.

2. Experimental procedure

Single crystals were grown by the conventional RF-heating Cz technique using iridium crucibles with a 50 or 150 mm diameter and height. The starting materials were prepared by mixing 99.99% pure oxide or carbonate powders in a stoichiometric ratio. The powders were mixed in air, and then calcined at 1000 °C for 2 h. They were heated at 1200–1300 °C for 2 h. The calcined powders were then pressed uniaxially in a disk form with a 48 mm diameter and ~30 mm thickness, and were charged into the crucible. The growth atmosphere was Ar gas flowing at 10^{-3} m^3/min. The pulling rate and the rotation rate were 2.0–3.0 mm/h and 20 rpm, respectively. The observation of bubbles and inclusions in the crystals was performed using an optical microscope. The phase identification of the as-grown crystals was determined by powder X-ray diffraction (XRD). The chemical composition was determined by inductively coupled plasma emission spectrometry (ICP-ES) analysis. The density of the grown crystals was measured by Archimedes method using distilled water at room temperature.

The dielectric, piezoelectric, and elastic compliance constants of the single crystals were determined using a YHP 4194A impedance/gain phase analyzer. Equivalent resonators were fabricated in the form of bars or plates. The electromechanical coupling factor and the piezoelectric modulus were evaluated by measuring the resonant and anti-resonant frequencies of these resonators in the length-extensional and thickness-shear modes.

Plate specimens with a 1 mm thickness and 20 mm width were prepared. The surface of the crystal was polished to be optically flat, while a lapping treatment was used for the other side. Al interdigital transducers (IDTs) were fabricated on the polished surface of the crystals by a photolithography process. A pair of IDTs was used for the filter measurement. The IDTs were placed on the crystals at 22.5° intervals of azimuthal angle, and the dependence of the SAW characteristics on the propagation direction was examined. The *S*-parameters of the IDTs were measured using a network analyzer (Advantest R3762AH), and the radiation admittance and filter characteristics were obtained. From these characteristics, the SAW velocity, v, and electromechanical coupling coefficient, k^2, were calculated. In order to obtain the temperature coefficients of the time delay (TCD), the temperature dependence of the frequency was also measured from 5 to 45 °C in 5° increments.

Fig. 1. As-grown (a) $La_3Ga_5SiO_{14}$, and (b) $Nd_3Ga_5SiO_{14}$ single crystals.

3. Results and discussion

3.1. RGS-type crystals

Fig. 1 shows typically grown (a) LGS and (b) $Nd_3Ga_5SiO_{14}$ (NGS) single crystals, pulled in the <0 0 1> direction. The grown crystals had a smooth crystal surface, and were transparent. The colors of LGS and NGS are orange and dark purple, respectively. No crack and inclusions were observed in the grown crystals. From the results of the phase identification, it was clarified that the grown crystal consisted of the *R*GS-type single phase. The densities of the grown crystals were 5.74 g/cm^3 for LGS and 6.01 g/cm^3 for NGS.

Table 1 shows the electromechanical coupling factors, k_{ij}, and piezoelectric constants, d_{ij}, of the LGS and NGS single crystals. All the factors and the constants of the LGS sample are greater than those of NGS. Fig. 2 shows the dependence of the piezoelectric modulus, d_{11}, on the lattice parameter, a, in the *R*GS-type crystals. The d_{11} data were collected from the literature ($Pr_3Ga_5SiO_{14}$ [10], $La_3Nb_{0.5}Ga_{5.5}O_{14}$ [11], $La_3Ta_{0.5}Ga_{5.5}O_{14}$ (LTG) [12], $La_3Al_xGa_{5-x}SiO_{14}$ [13], $Sr_3Ga_2Ge_4O_{14}$ [14] and $Na_2CaGe_6O_{14}$ [15]). As can be seen from Fig. 2, an increase in the lattice parameter, a, leads to an increase of the piezoelectric modulus, d_{11}. This tendency can be explained as follows: Increasing the lattice parameter a means enlarging the size of the polyhedra composed of a cation and the nearest oxygens along the a-axis. The

Table 1
Electromechanical coupling factor k_{ij} and piezoelectric constant d_{ij} of the LGS and NGS crystals

Crystals	Coupling factor (–)			Piezoelectric constants (pC/N)	
	k_{12}	k_{25}	k_{26}	d_{11}	d_{14}
LGS	0.148	0.089	0.138	5.95	−5.38
NGS	0.097	0.029	0.121	4.05	−2.07

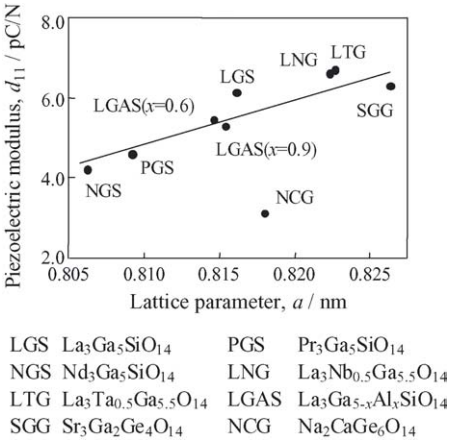

Fig. 2. Piezoelectric modulus, d_{11}, vs. lattice constant, a, of *R*GS-type crystals.

d_{11} modulus of the crystal with trigonal symmetry signifies a magnitude of electric charge developed by the applied stress along the crystallographic a-axis. By such an enlargement, the cations can move more easily within the crystal. Thus, even if the applied stress is relatively small, the polarizations could easily increase. In Fig. 2, the small d_{11} value of $Na_2CaGe_6O_{14}$ may be caused by the features of crystal structure as follows: (1) the coordination around both tetrahedral sites; and (2) the displacement ellipsoids for the oxygen atoms of $Na_2CaGe_6O_{14}$ are apparently different from those of the other *R*GS-type crystals [15].

The LGS crystal belongs to the trigonal system, point group 32, and is a compound isostructural to $Ca_3Ga_2Ge_4O_{14}$ [16]. Fig. 3 shows the schematic coordination polyhedra of oxygen atoms around the cationic atoms in the *R*GS-type structure. There are four kinds of cation sites in this structure, and this structure can be represented by the chemical formula, $A_3BC_3D_2O_{14}$. In this chemical formula, A and B represents the decahedral (twisted Thomson cube) site coordinated by eight oxygen anions, and an octahedral site coordinated by six oxygen anions, respectively. While both C and D represents a tetrahedral site coordinated by four oxygen anions, the size of the D site is slightly smaller than that of the C site.

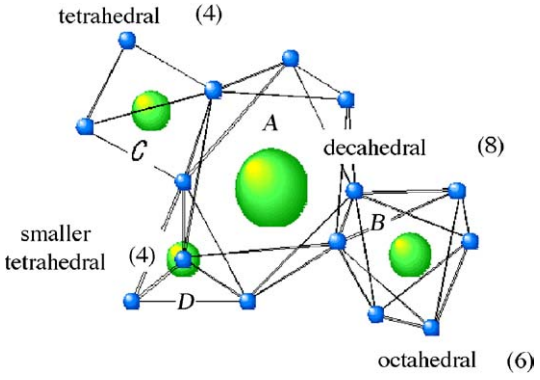

Fig. 3. Schematic coordination polyhedra of oxygen atoms around cationic atoms in *R*GS-type structure. Small circles represent oxygen atoms.

For the LGS single crystal, La^{3+} occupies the A site, Ga^{3+} occupies B, C and half of the D sites, and Si^{4+} half of the D site. We determined the ionic size preferences of the cation sites in the *R*GS-type structure. Fig. 4 shows the structure stability diagrams of the (a) A-site, (b) B-site, (c) C-site, and (d) D-site in the *R*GS-type crystal structure. The ionic radius values were the data reported in Ref. [17]. In this study, we defined the structure stability as an index of the site preference of a cation. The diagrams in Fig. 4 were fabricated by modifying the stability diagram of the *R*GS-type structure [18] using the crystal structure analysis data [10,15,16,19]. The stability diagram in Ref. [18] was also prepared using the data for the synthesis for the *R*GS-type crystals reported in Refs. [20,21]. In Fig. 4, it means that a cation showing a high structure stability is easy to form the RGS-type crystal and to incorporates a corresponding site in the structure. From Fig. 4(a)–(d), the element and ionic size preferences of the cation sites in the *R*GS-type structure are summarized as follows:

$$\begin{aligned} A &= Na^{+},\ Sr^{2+},\ La^{3+} \quad (\text{c.a. } 0.122\,\text{nm}),\\ B &= Ga^{3+},\ Sn^{4+},\ Nb^{5+},\ Ta^{5+} \quad (\text{c.a. } 0.065\,\text{nm}),\\ C &= Ga^{3+},\ Ge^{4+} \quad (\text{c.a. } 0.043\,\text{nm}),\\ D &= Si^{4+},\ Ge^{4+},\ Al^{3+} \quad (\text{c.a. } 0.033\,\text{nm}) \end{aligned} \tag{1}$$

Based on the information derived from the data in Figs. 2 and 4, we first synthesized the $Sr_3TaGa_3Si_2O_{14}$ single crystals. The electromechanical coupling factor, k_{ij}, of this crystal was comparable to that of LTG with the highest k_{ij} values [12]. Moreover, we synthesized new *R*GS-type $Ba_3TaGa_3Si_2O_{14}$ (BTGS) single crystals. The crystals had a smooth surface, and were transparent and colorless. Although many bubbles were observed in the center parts of the crystal, we fabricated a Y-cut wafer for the SAW measurements as shown in Fig. 5. The crystal structure of BTGS was analyzed using the single-crystal X-ray diffraction data. The results showed that the Ba, Ta, Ga, and Si atoms occupy their respective crystallographic A, B, C, and D sites in an ordered way, respectively. The SAW properties of BTGS were also investigated. The maximum k^2 values in the Y-cut BTGS wafer was about 0.43% for the x-axis propagation. This value is greater than those of LGS (0.38% [22]) and LTG (0.39% [23]). For the BTGS crystal, a large reduction (40–45%) in the Ga_2O_3 amount versus LGS and LTG is expected. The piezoelectric device made of the BTGS crystal allows the use of a lower amount of expensive gallium oxide as the raw material.

3.2. RCOB crystals

Fig. 6 shows typically grown (a) LaCOB and (b) $Gd_xY_{1-x}Ca_4O(BO_3)_3$ (GdYCOB) single crystals pulled in the <0 1 0> direction. The <0 1 0> pulling direction is perpendicular to the mirror plane in the crystal. Both crystals have

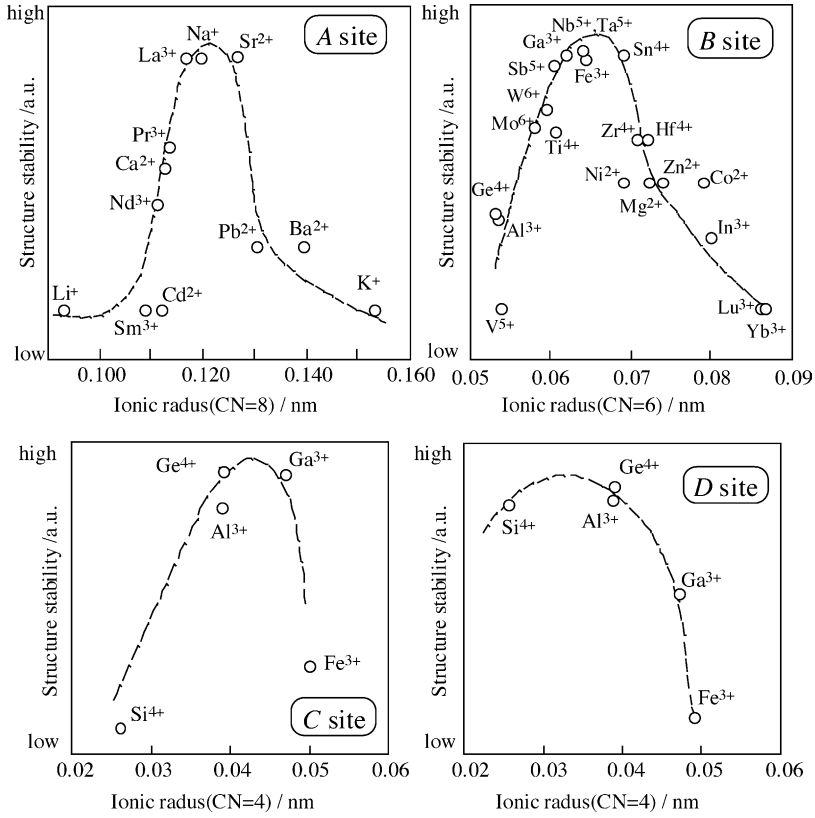

Fig. 4. Structure stability diagram of the (a) *A*-site, (b) *B*-site, (c) *C*-site, and (d) *D*-site in the *R*GS-type crystal. CN denotes the coordination number. Ionic radius data in nm are given by converting those in Å in Ref. [20].

a smooth crystal surface, and are transparent and colorless. No inclusions and bubbles were observed in the crystals. The shape of the boule was a quadrilateral prism, which consisted of planes parallel to $\{1\,0\,1\}$ and $\{2\,0\,\bar{1}\}$. Furthermore, the $\{0\,1\,0\}$ facet is observed on the solid–liquid interface at the bottom of the crystal. The facet on the solid–liquid interface was connected to a core formed during the *R*COB crystal growth [24]. An X-ray powder diffraction analysis confirmed that all of the *R*COB grown crystals were composed of the *R*COB single phase. The chemical composition of the grown LaCOB crystals was determined by ICP-ES. The composition was almost uniform from the top to the bottom of the crystal, and the same as the melt in the crucible. We

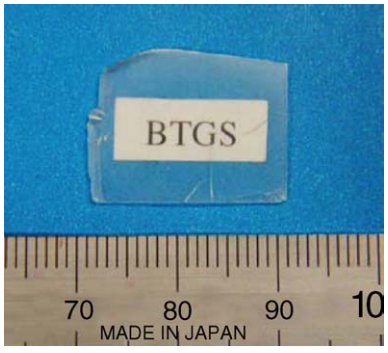

Fig. 5. Y-cut wafer of $Ba_3TaGa_3Si_2O_{14}$ crystal.

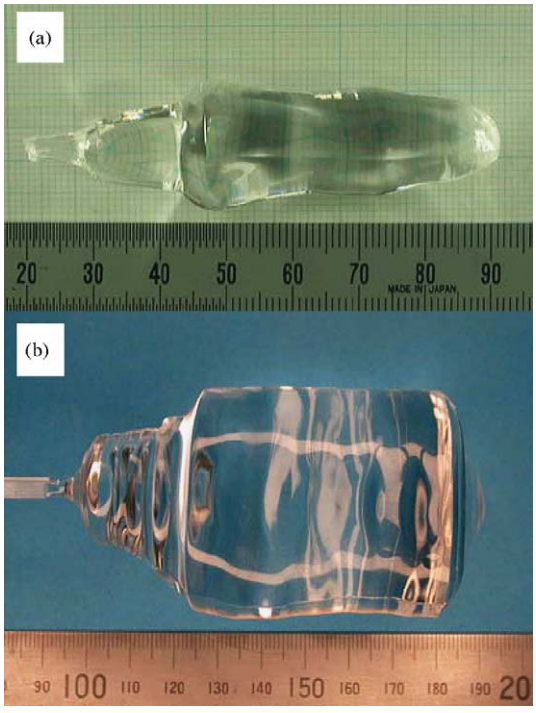

Fig. 6. As-grown (a) $LaCa_4O(BO_3)_3$, and (b) $Gd_xY_{1-x}Ca_4O(BO_3)_3$ single crystals.

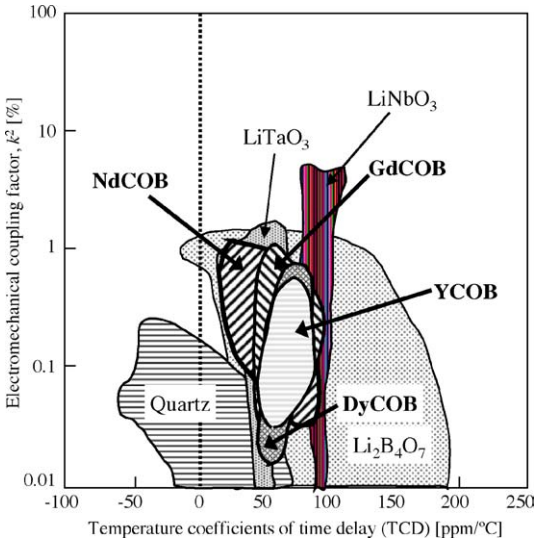

Fig. 7. Electromechanical coupling factors, k^2, vs. temperature coefficient of delay (TCD) in RCa$_4$O(BO$_3$)$_3$-type crystal including other piezoelectric materials.

obtained the same results on other *R*COB crystals, in which *R* consisted of only one element [25]. Therefore, we consider that the *R*COB crystals congruently melt. In the GdYCOB crystal, we observed continuous changes with the composition and crystallographic parameters along the growth axis. The GdYCOB crystal shown in Fig. 6(b) was grown with a 3.0 mm/h-pulling rate. In spite of the difficult conditions for crystal growth, we obtained a high quality GdYCOB crystal. Therefore, the bulk *R*COB crystals can be grown by the Cz technique, and this result is a great advantage for mass-production.

Fig. 7 shows the k^2 and TCD behaviors in the *R*COB-type crystals along with other piezoelectric materials. Those of quartz, $Li_2B_4O_7$, $LiNbO_3$ and $LiTaO_3$ are listed using Ref. [26,27]. Both high k^2 and low TCD values are important factors for the SAW device. The highest k^2 of 1.0% and lowest TCD of about 5 ppm/°C of all the *R*COBs were from in the NdCOB crystal. This TCD value was equivalent to a quartz crystal and the k^2 value is nearly ten times greater than that of the quartz. The SAW properties shown in Fig. 7 were obtained on the *X*-, *Y*- and *Z*-cut substrates of the *R*COB crystals. The SAW parameters (wave propagation and cut directions) with high k^2 and low TCD value can be optimized by a numerical simulation when the material constants (dielectric, piezoelectric, and elastic compliance constants) and their temperature coefficients are evaluated. Mason has reported the crystal substrates for measuring the material constants of point group 2 [28], however, there are few numerous experimental and theoretical studies concerning those of point group *m*, i.e., the crystal symmetry of *R*COB. We also tried to establish how to measure the material constants and have been reporting some of them [29,30]. The more detailed SAW characterization, as well as the evaluation of the material constants are under investigation. The *R*COB crystals are expected to be application-competitive materials with the quartz or $LiNbO_3$, which is widely used in existing devices.

4. Summary

Rare-earth element-based piezoelectric single crystals, *R*GS (*R* = La and Nd) and *R*COB (*R* = La, Nd, Gd, Dy, and Y), were grown by the Czochralski technique. The piezoelectric properties of the *R*GS and *R*COB crystals were investigated. For the *R*GS-type crystal, the relationship between the crystal structure and piezoelectric properties was determined. It was found that the *R*GS-type crystals with the largest lattice parameter have the highest piezoelectric constants. The cation stability in the *R*GS-type crystal was also discussed. The cation stability diagrams were constructed on the basis of many *R*GS-type crystal syntheses. Based on these results, a new *R*GS-type BTGS crystal was synthesized and its SAW properties were investigated. We obtained a high k^2 value than those of LGS and LTG. In the *R*COB-type crystal, large GdYCOB single crystals up to 2 in. in diameter were easily grown. The SAW properties of the *R*COB filters were also measured. We found that the NdCOB single crystal has the highest k^2 and lowest TCD values of the *R*COB crystals. The SAW properties were intermediate between those of the existing quartz and $LiNbO_3$ crystals. We expect that the *R*GS and *R*COB-type crystals will be the preferable piezoelectric materials for SAW devices.

References

[1] K. Yamanouchi, M. Takeuchi, T. Meguro, Y. Wagatsuma, Electron. Lett. 21 (1985) 966.
[2] M. Adachi, T. Shiosaki, A. Kawabata, Jpn. J. Appl. Phys. 24 (1985) 72.
[3] A.N. Gotalskaya, D.I. Drezin, V.V. Bezdelkin, V.N. Stassevich, Proc. IEEE Freq. Symp. 47 (1993) 339.
[4] E. Philippot, A. Ibanez, Proc. 1992 IEEE Int. Freq. Control Symp., p.744.
[5] T.N. Khamaganova, V.K. Trunov, B.F. Dzhurinski, Russ. J. Inorg. Chem. 36 (1991) 484.
[6] R. Norrestam, M. Nygren, J.O. Bovin, Chem. Mater. 4 (1992) 737.
[7] G. Aka, A. Kahn-Harari, D. Vivien, J.M. Benitez, F. Salin, J. Godard, Eur. J. Solid State Inorg. Chem. 33 (1996) 727.
[8] M. Iwai, T. Kobayashi, H. Furuya, Y. Mori, T. Sasaki, Jpn. J. Appl. Phys. 36 (1997) 276.
[9] J.J. Adams, C.A. Ebbers, K.I. Schaffers, S.A. Payne, Opt. Lett. 26 (2001) 217.
[10] J. Sato, H. Takeda, H. Morikoshi, K. Shimamura, P. Rudolph, T. Fukuda, J. Cryst. Growth 191 (1998) 746.
[11] I.M. Sil'vestrova, Yu.V. Pisarevskii, A.A. Kaminskii, B.V. Mill, Sov. Phys. Solid State 29 (1987) 870.
[12] Yu.V. Pisarevsky, P.A. Senyushenkov, B.V. Mill, N.A. Moiseeva, IEEE Trans. Ultrason. Freq. Control 45 (1998) 742.
[13] M. Kumatoriya, H. Sato, J. Nakanishi, T. Fujii, M. Kadota, Y. Sakabe, J. Cryst. Growth 229 (2001) 289.
[14] V.V. Kochurikhin, M. Kumatoriya, K. Shimamura, H. Takagi, T. Fukuda, J. Cryst. Growth 181 (1997) 452.

[15] H. Takeda, R. Uecker, M. Kumatoriya, K. Shimamura, P. Reiche, T. Fukuda, Crys. Res. Tech. 32 (1997) 939.
[16] B.V. Mill, A.V. Butashin, G.G. Khodzhabagyan, E.L. Belokoneva, N.V. Belov, Dokl. Akad. Nauk. SSSR 264 (1982) 1385.
[17] R.D. Shannon, Acta Crystallogr. A 47 (1976) 751.
[18] Y.M. Yu, V.I. Chani, K. Shimamura, T. Fukuda, Mater. Sci. Eng. R 20 (1997) 281.
[19] (a) H. Takeda, T. Kato, V.I. Chani, H. Morikoshi, K. Shimamura, T. Fukuda, J. Alloy Compd. 290 (1999) 79;
(b) H. Takeda, T. Kato, V.I. Chani, K. Shimamura, T. Fukuda, J. Alloy Compd. 290 (1999) 246;
(c) H. Takeda, J. Sato, H. Morikoshi, T. Kato, K. Shimamura, T. Fukuda, Mater. Lett. 41 (1999) 104;
(d) H. Takeda, M. Kumatoriya, T. Shiosaki, Appl. Phys. Lett. 79 (2001) 4201;
(e) H. Takeda, R. Aoyagi, S. Okamura, T. Shiosaki, Ferroelectrics 295 (2003) 67.
[20] B.V. Mill, A.V. Butashin, G.G. Khodzabagyan, E.L. Belokoneva, N.V. Belov, Sov. Phys. Dokl. 27 (1982) 434.
[21] B.V. Mill, A.V. Butashin, A.M. Ellern, Inorg. Mater. 19 (1983) 1516.
[22] T. Sato, A. Nishikata, Y. Shimizu, Jpn. J. Appl. Phys. 36 (1997) 3068.
[23] N. Onozato, M. Adachi, T. Karaki, Jpn. J. Appl. Phys. 39 (2000) 3028.
[24] H. Furuya, M. Yoshimura, I. Yamada, H. Nakao, Y. Mori, T. Sasaki, J. Jpn. Assoc. Crystal Growth 25 (1998) 3 (in Japanese).
[25] H. Nakao, M. Nishida, T. Shikida, H. Shimizu, H. Takeda, T. Shiosaki, J. Alloy Compd. 408–412 (2006) 582–585.
[26] S. Miyazawa, Kogaku Kessho, Baifukan, Tokyo, 1995, pp. 7–8 (in Japanese).
[27] Y. Shimizu, H. Shimizu, M. Koshiba, Y. Yamamoto, in: M. Shibayama (Ed.), Dansei-ha Soshi Gijyutsu Handbook, Ohm-sha, Tokyo, 1994, pp. 148–184.
[28] W.P. Mason, Phys. Rev. 70 (1946) 705.
[29] H. Takeda, H. Sako, H. Shimizu, K. Kodama, M. Nishida, H. Nakao, T. Nishida, S. Okamura, T. Shikita, T. Shiosaki, Jpn. J. Appl. Phys. 42 (2003) 6081.
[30] H. Shimizu, K. Kodama, H. Takeda, T. Nishida, T. Shikita, S. Okamura, T. Shiosaki, Jpn. J. Appl. Phys. 43 (2004) 6716.